Understanding Fluid Flow to Improve Lubrication Efficiency

Haruo Houjoh, Shun-ichi Ohshima, Shigeki Matsumura, Yasuhiro Yumita, Keiji Itoh

Abstract

Excess lubricant supply in gearing contributes to power loss due to churning as well as the requirements of the lubrication system itself. Normally, a much larger amount of oil than required is used for cooling because so much of it is thrown away by centrifugal force. To lower the amount of lubricant required and reduce those losses, it is necessary to discover the ideal location of the supplying nozzle. The authors have measured the pressure variation during the mesh process, which will give us an idea of how we can deliver the lubricant with minimal but efficient cooling. Pressure measurement was done for several pairs of helical gears that have gages installed at the bottom of the root space. A sucking action is found to distribute lubricant along the tooth mesh, especially at the recess side of meshing. Although there is a global axial flow due to the helix angle, which is directed from the leading side towards the trailing side, the opposite flow exists partially at the trailing side.

Table 1—Dimensions of tested gears.

Gear ID		S	H1	H2	H3	H4
Helix angle (deg.)	b	0	13	16	21	30
Number of teeth	z	76	74	73	71	66
Normal module	m_n	4				
Pressure angle (deg)	α_n	20				
Face width (mm)	b	100				
Center distance (mm)	a	304				
Outer diameter (mm)	d_a	312				
Contact ratio		1.82	3.44	3.77	4.28	5.09

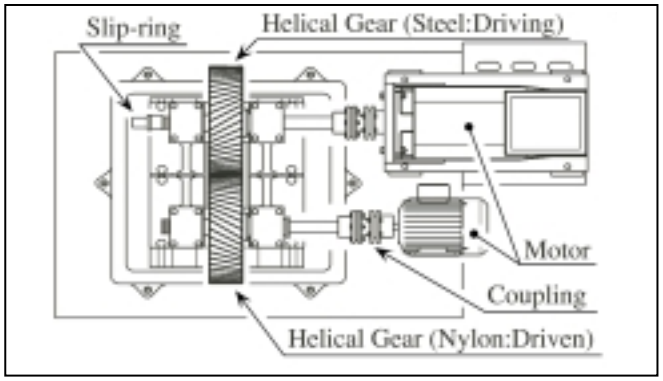

Figure 1—Gear arrangement for pressure measurement.

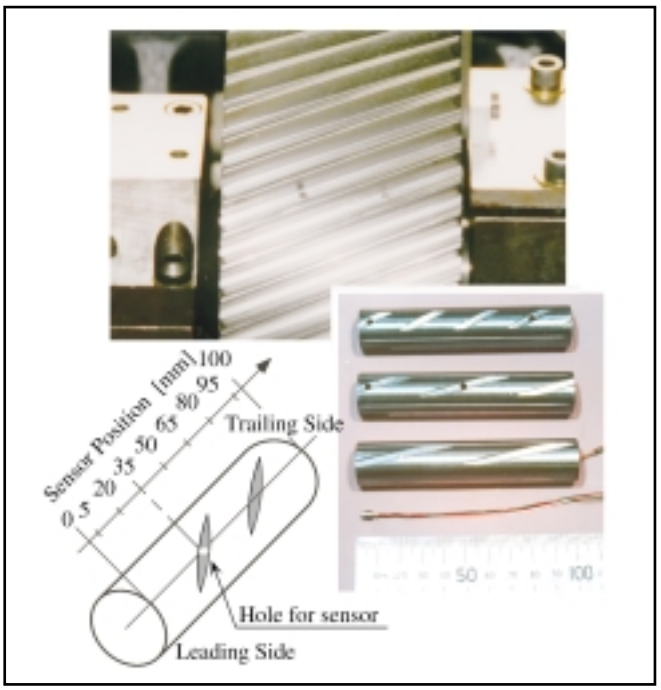

Figure 2—Appearance of rods and gear with rods at the bottom of teeth.

Introduction

Social requirements for energy saving are forcing various efforts to reduce excess power losses of mechanical elements. For a gear reducer, auxiliary consumption may be due to lubrication systems, windage, etc. Several solutions have been proposed by gear manufacturers. Renk AG is now utilizing a vacuum chamber to reduce windage loss (Ref. 1) while D.D. Winfree describes a method of decreasing windage loss by applying a baffle close to the tooth tip (Ref. 2). Since there are quite a few kinds of gear reducers, the solution must not be unique to just one kind.

Although the lubricant is expected to cool the tooth surface just after meshing, most of it does not work as expected because the lubricant is cast or thrown away by a strong centrifugal force before tooth engagement occurs. If one feeds the oil from the mesh entrance, most of it will get out before the mesh action. It is only vaguely known whether feeding the oil from the mesh exit works for both lubrication and cooling. These arguments have existed since the early stages in gear technology. However, the optimal way to avoid energy loss by reducing the amount of oil is still uncertain.

With a main focus on cooling the tooth, it is necessary to observe the behavior of the medium around the mesh region and find a way to deliver the oil to the appropriate position. This depends on the pitch line velocity, but the authors have found some strong pumping and suction effects, even at operating speeds of less than 50 m/sec. Accordingly, the present work will provide a database of dynamic air behavior, which closely correlates the oil delivery. The behavior at the mesh end region is mainly observed since it is important to feed enough oil there to cool the tooth surface.

The authors have already presented the behavior for a pair of spur gears (Ref. 3). Although the result was quite interesting, it seemed difficult to utilize the results for practical gearing since the air gets into the tooth space from both ends as a one-dimensional flow and collides at the middle of the tooth width. On the

contrary, observation of a helical gear pair seems quite valuable since axial pumping action is expected to assist delivery of oil to the full surface.

Experimental Condition

Tested Gears. Four gear pairs were prepared to measure the pressure fluctuation at the tooth space bottom with different helix angles as shown in Table 1. Gears were assembled as shown in Figure 1 for pressure measurement. Each pair consists of a steel gear as a driver for pressure measurement and a nylon gear as a follower for dry operation. Every steel gear has left-hand helix angles, while the nylon gears have right-hand helix angles. For pressure measurement, cylindrical rods were embedded into a steel gear body aligned parallel to the axis so that a part of its skin conforms to part of the tooth space bottom.

Pressure Measurement Rod. For this purpose, rods were inserted to pre-bored holes before hobbing the gear blanks. Then, teeth were fabricated by hobbing, along with tangential shifts, to have narrower tooth thicknesses so that the bottom of a tooth space has sufficient width for exposing the pressure gage surface properly. Afterwards, the rods were removed and machined to attach the pressure gage so that the sensing surface was in the same plane as the bottom surface. Four or five rods were embedded in one gear body in such a position that the measurement could be done at desired places distributed width-wise over the length of the tooth space.

As shown in Figure 2, the measurement positions of the sensors were designed to be approximately b = 5, 20, 35 and 50 mm axially distant from the leading edge of the tooth space. Because of symmetry in the rotating direction, b can also equal 95, 80, 65 and 50 mm respectively under reverse rotation. Semiconductor press gages with a 3 mm diameter were used and embedded in the rod. Then the sensor surface becomes part of the bottom of the space and measures gage pressure. The sensor could measure transient behavior with resonance frequencies higher than 50 kHz.

Measurement

A schematic measurement system is presented in Figure 3. The pressure signal was fed through a slip ring at the end of a shaft to an FFT analyzer, and it averaged the signal synchronously to a once-per-revolution trigger signal. The number of averaging was determined 256 times to eliminate variation and system noise.

Measured pressure fluctuation can be presented in terms of two kinds of angular positions of a gear—the first is the angular position of individual pressure sensors that demonstrate behavior in accordance with the rotation of tooth space on the traverse cross-section, including the sensor. The other presents the behavior against the gear body, which corresponds to the dependence on time and medium motion. In this paper, the latter expression is used and represented by the angular sensor position of b = 5 mm. Figure 4 indicates the angular movement graphically to assist in better understanding the geometry.

Experimental Results

Figure 5 shows gage pressure vs. angular movement of a driving gear for the case where the helix angle is $\beta = 13°$ at the speed of 3,780 rpm (about 60 m/sec) of pitch line velocity. The

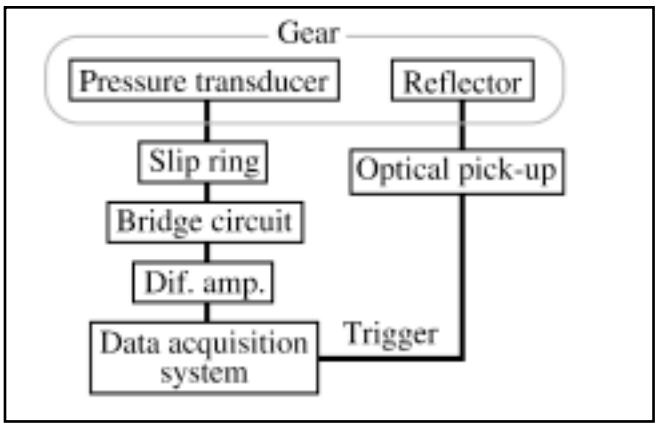

Figure 3—Schematic diagram of measurement procedure.

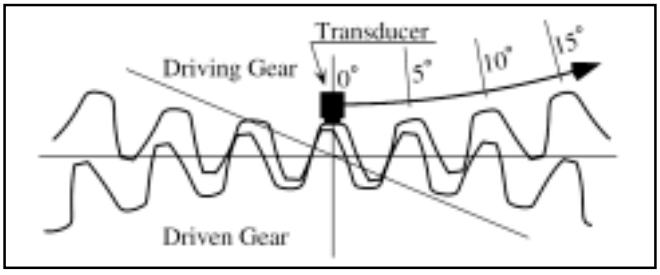

Figure 4—Geometry of pressure sensor installation from axial view.

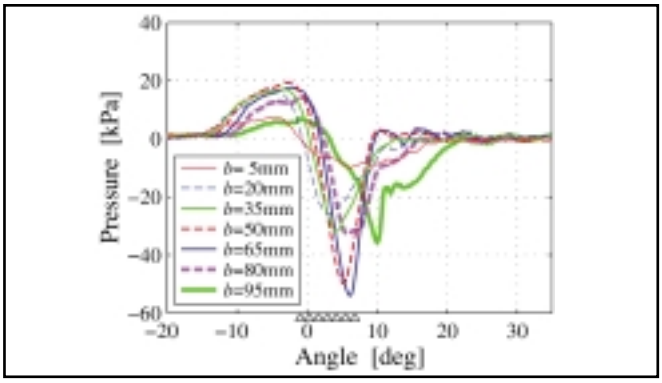

Figure 5—Time dependence of pressure at tooth space for a helical gear pair ($\beta = 13°$); Triangles at the bottom of abscissa show the position of the minimal cross-sectional area of individual pressure measurement.

Dr. Haruo Houjoh *has been involved in discovering sound generation by air pumping during the mesh process and in gear dynamics since 1976. He is currently employed as a professor at the Tokyo Institute of Technology.*

Shun-ichi Ohshima *has been an assistant professor at the Tokyo Institute of Technology since 1994. His area of expertise is in acoustic measurement technology with a 2-D microphone array and experimental visualization.*

Dr. Shigeki Matsumura *is an associate professor at Tokyo Institute of Technology. He is credited with developing a dynamic simulator for a pair of helical gears under partial load conditions.*

Yasuhiro Yumita *is a project engineer at East Japan Railway Co. His area of focus is in pressure measurement.*

Keiji Itoh *is an engineer at Mitsubishi Heavy Industries Ltd. Itoh specializes in the visualization of oil delivery by using an oil droplet shot via a custom-made electric gun.*

horizontal axis indicates the angular position of a sensor placed at b = 5 mm. The small triangles on the horizontal axis mark the points where the center of backlash of each transverse cross section passes across the pitch point height.

Pressure rise begins at the leading end of the tooth space b = 5 mm, and it is followed by consequential pressure rise point-by-point to the trailing end. The pressure fluctuation is not strong at the leading end, and the trailing end's fluctuation is different from others. This weakness must be due to the boundary effect of tooth ends. Pressure curves at the inner locations have phase lag that corresponds to the helix angle. Basically, individual pressure increases gradually as the space goes through meshing and becomes higher at one pitch before the sensor passes through the pitch point height. The maximum is hereafter called "positive peak."

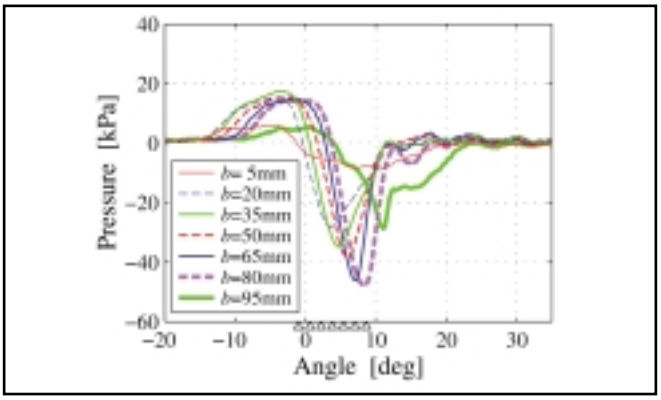

Figure 6—Time dependence of pressure at tooth space for a helical gear pair (β = 16°). Triangles at the bottom of abscissa show the position of the minimal cross-sectional area of individual pressure measurement.

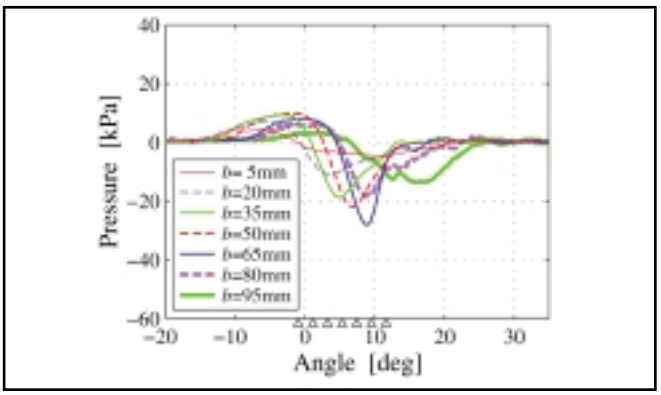

Figure 7—Time dependence of pressure at tooth space for a helical gear pair (β = 21°). Triangles at the bottom of abscissa show the position of the minimal cross-sectional area of individual pressure measurement.

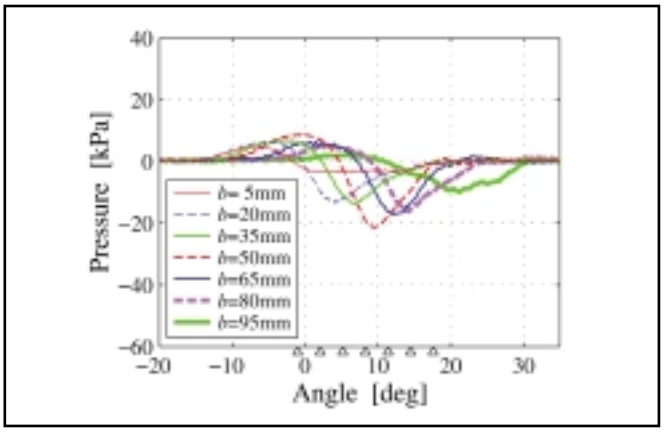

Figure 8—Time dependence of pressure at tooth space for a helical gear pair (β = 30°); Triangles at the bottom of abscissa show the position of the minimal cross-sectional area of individual pressure measurement.

The maximum pressure seems independent of sensor position except at both ends. After reaching the maximum pressure, it then switches from positive to negative when the center of the backlash cross section passes along the pitch point height. Negative pressure becomes lower when the sensor passes across the pitch point. This is called the "negative peak," which occurs when the backlash space passes along the pitch point height. Both representative points slightly differ from each other with respect to peak magnitude and timing, both of which are dependent on sensor position.

The negative pressure is remarkably strong when compared to positive pressure. It is exceptionally strong at the points of both b = 50 and 65 mm. The pressure fluctuation resembles the results of spur gear tests presented by the authors from the aspect of global view. In addition, there is a specific pressure fluctuation at the trailing end b = 95, where the negative peak position is hardly found because it lasts for a certain period, which seems independent of the formerly described peak.

The results of other gears are shown in Figures 6–8. The basic shape of pressure variations is almost the same except for the magnitude. As the helix angle increases, the pressure becomes smaller and spacing of traces become wider due to larger lag times between adjacent sensing sections.

Discussions

Dependence of pressure on speed. From Figures 5–8, positive and negative peak pressures were read from the temporal traces and plotted on Figure 9 for two types of gears β = 13° and 30°. It is obvious that the peak pressure (absolute value) is proportional to the square of speed for both positive and negative. This quadratic tendency is naturally understood from the viewpoint of compressible fluid dynamics. Previous studies for a spur gear indicated this same tendency.

Dependence of pressure on helix angle. It is also clear that the peak pressure decreases as the helix angle increases. The negative peak pressure is much stronger than the positive one. It is supposed that the positive peak pressure at the entrance of engagement will refuse the oil delivery. On the contrary, negative pressure at the end of the engagement will help the oil delivery reach the tooth surface after meshing. This will be available only for effective cooling on the surface, not for friction reduction, because the oil must be thrown away by the centrifugal force.

Temporal and spatial behavior of pressure fluctuation. The pressure variation at the bottom of the tooth space indicates nothing but the pressure. Then, it is necessary to grasp the pressure fluctuation versus time in a 3-D space and imagine the motion of the medium.

Figure 10 shows the results compiled from the pressure measurement in Figure 6, β = 13°, 3,780 rpm. Each plot indicates the instantaneous pressure distribution along the tooth space. Angles presented at the left side indicate the angular movement of the gear in terms of the position of the pressure sensor placed at 5 mm interior from the leading end face of the gear. The negative angles indicate the region where the space is approaching the mesh, and therefore the angular position of –1° means that the tooth space of the driving gear at b = 5 mm is at the position before passing the pitch point height.

Oblique lines are the timing of backlash space passage at individual transverse cross sections where, as shown in Figure 11, mating (driven) tooth tips just enter the tooth space or invade the tip circle; preceding working tooth surfaces of the tooth space finish engagement; working surface of the tooth space enters mesh and the backlash space is isolated from the adjacent space; the sole backlash space is at its minimum; the preceding working surface finishes engagement; working surface of the tooth space finishes engagement; and mating tooth tips leave the tooth space boundary (tip circle of driving gear).

Negative pitch pressures occur just before the space bottom passes through the pitch point height. It travels from the leading end toward the opposite end with negatively growing pressure. However, the negative peak position follows the axial travel of tooth contact with a small lag, depending on the sensor location. It is assumed that the suction travels continuously by drawing the air from the leading area. Pressure becomes maximum at b = 65 mm. Then the peak pressure disappears before reaching the end of the face width. Instead, another negative peak grows at the trailing end and it does not move, but the magnitude does vary.

For the gear with helix angle β = 30°, as shown in Figure 12, the negative pressure region travels uni-directionally from the leading to the trailing end. The result indicates that, if the oil is fed so it has an axial velocity component or oblique incident, then it can be properly delivered with the aid of suction produced by the gear itself.

These phenomena suggest that there are two features: One is similar to a spur gear pair, in which air comes into the tooth space from both ends of tooth width. The other is specific for a helical gear, in which air travels uni-directionally due to axial movement of instantaneous tooth-to-tooth contact area.

The result indicates that if the oil is fed from the recess side, it is first sucked into the tooth space. Since the negative peak travels along the tooth space, oil will get deep into the tooth space in the actual direction. Therefore, it should be fed with axial velocity from the leading edge toward the trailing end. The reason is, axial movement of medium is mainly dependent on phase difference of mesh geometry between the leading end and the trailing end of helical gears, or on overlap ratio. This means if the helix angle is small but the face width is wide, the gear pair may be classified as "helical-like" rather than "spur-like." Therefore, movements of the helical gear pair can be utilized to assist lub delivery.

Visualization of Oil Delivery

To visualize the oil delivery, two kinds of experiments were conducted for the gear pair of β = 21°. One is shown in Figure 13 via a hand sketch after operating the gear pair for a certain length of time. The lubricant oil was manually fed with an oil

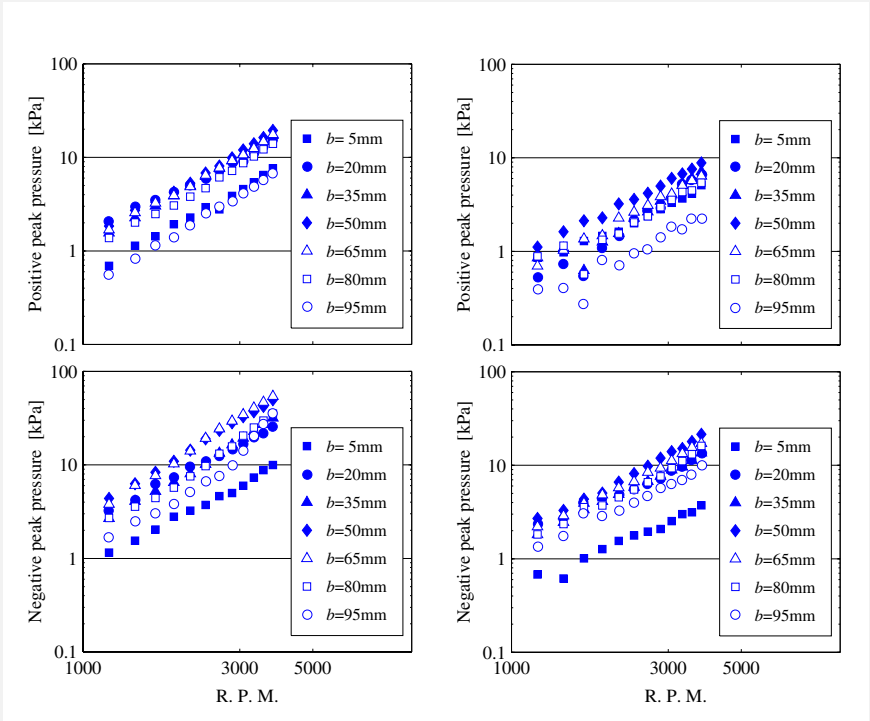

Figure 9—Dependence of representative pressure on gear speed (absolute peak value at both compression and sucking side); Left β = 13°, Right β = 30°.

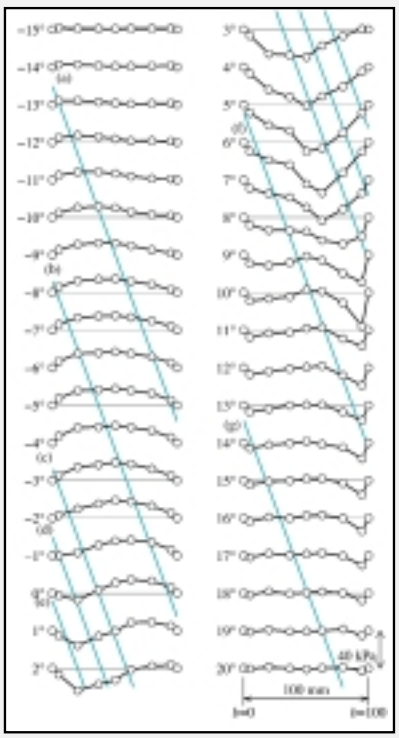

Figure 10—Pressure distribution along the tooth space vs. gear rotation (β = 13°).

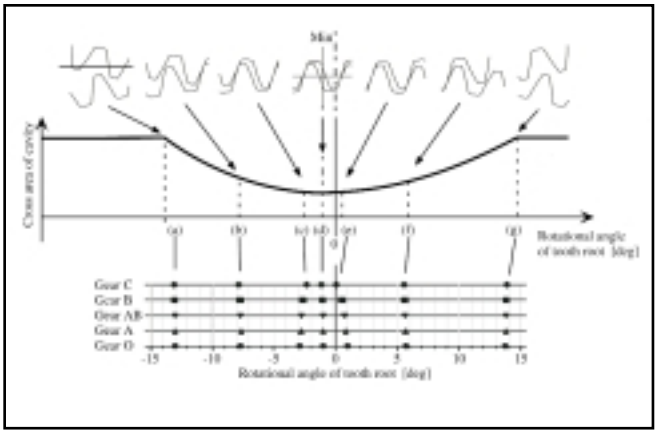

Figure 11—Angular movement of gear and geometry of mating teeth and space.

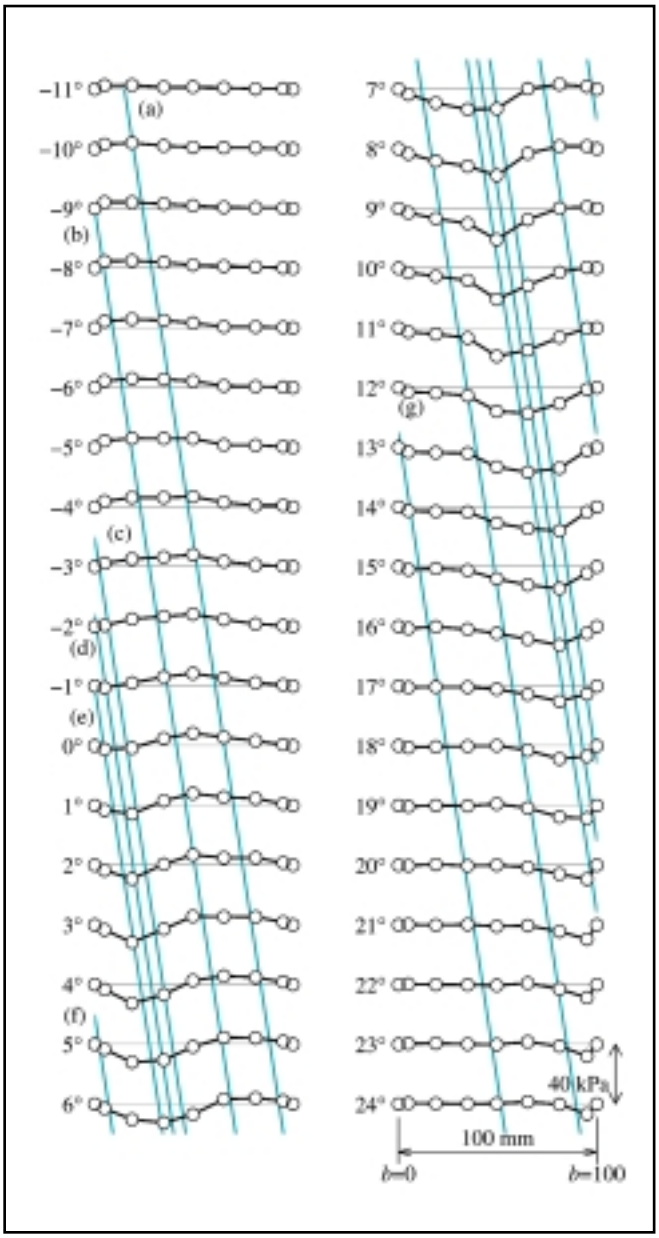

Figure 12—Pressure distribution along the tooth space vs. gear rotation ($\beta = 30°$).

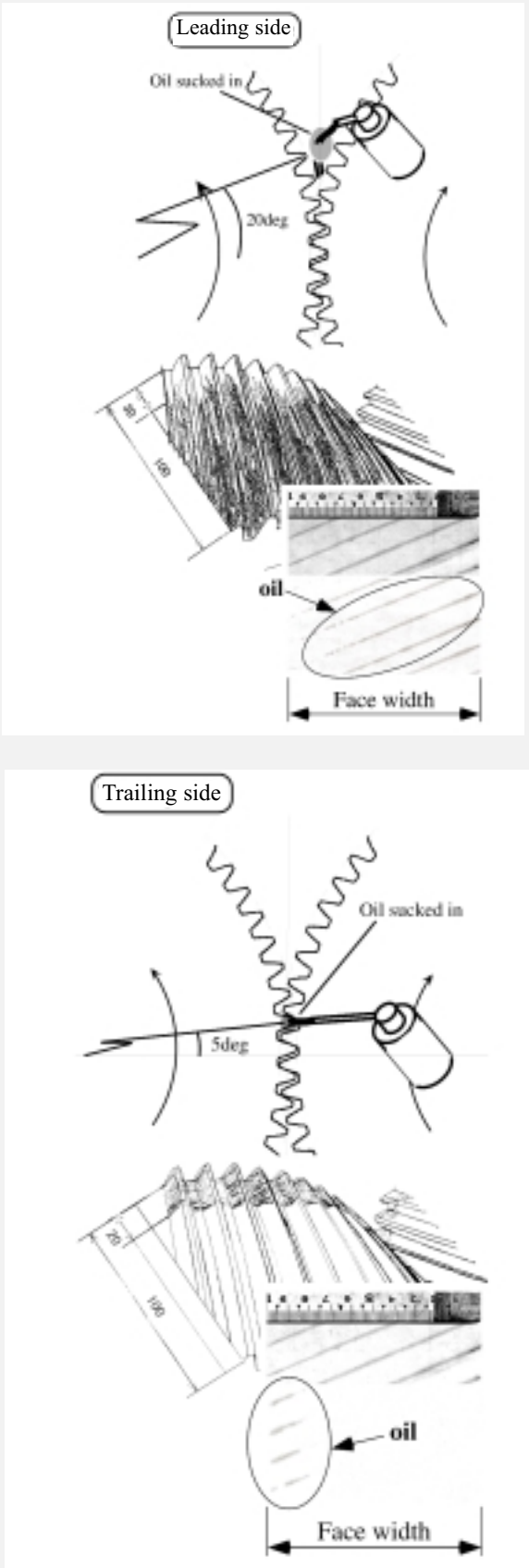

Figure 13—Hand sketch of oil supplied from both ends of the tooth space and the observed result of oil delivery; Top: fed from leading side, Bottom: fed from trailing side.

feeder as presented in the figure. At the exit of a nozzle, the oil had slightly more velocity when compared to the gear speed. Oil delivery was visually checked and then verified by printing the oily top of the teeth over paper. As seen in the figure, if an oil feed is at the recess region, oil reaches a certain longitudinal depth. However, it is clear that oil did not go across the whole face width. Instead, if the oil is fed from the trailing end, it reaches a depth where the oil did not make it from the opposite end.

Another experiment was done using an oil droplet, which was shot by an electric solenoid as drawn in Figure 14. The oil nozzle was designed such that a small amount of oil could be shot by the impacting action of the solenoid. The oil droplet was horizontally shot in an axial direction from the leading end of engagement and behind the intersection of tooth tip circles.

Figure 15 shows a result taken by printing the oily tooth tip land where the droplet was attached during the travel. The figure is presented by the contrast of the full width tooth stamp. The left-side figure is the result for a smaller amount of oil or higher initial speed velocity. The right-hand figure is the result for larger droplets, which means the initial velocity is slower. These results indicate that the oil droplet is flying over the intersecting line of two circumferential cylinders in the axial direction. There are two features recognized—a radial sucking action even though the tooth space has centrifugal action and an axial acceleration of the droplet since the right-hand figure shows the parabolic trace. It is unusual that, even at the recessing region, there is a strong force keeping the oil close to the gear.

Validity for Other Dimensions

It is difficult to experiment for various configurations such as different modules, different face widths, etc. Therefore, it is desirable to estimate the phenomena in a non-dimensional form. From the experience of acoustic measurement done by one of the authors for pumping action (Ref. 4), it is supposed that the dynamic behavior of the medium follows a parameter of b/λ where λ is the sound wavelength of tooth frequency.

This means the sound emission follows a similar law governed by the tooth face width and the size of a tooth or module. Module is implicitly included within the parameter λ, which is inversely proportional to mesh frequency. If one designs a gear pair with a fixed center distance or under the condition where the number of teeth times the module is constant, then mesh frequency is proportional to the number of teeth times revolution speed. This leads to the parameter $b*z*N/m$, which will determine the pressure in which the variation rate of space area is taken into consideration. Peak pressure will decrease as the helix angle increases.

The other estimate is spur- or helical-like characteristics of axial movement. For this argument, the authors think the parameter should include module and face width in addition to tooth angle. This is because the mating tooth affects movement of the medium. Therefore, if the helix angle is small but the face width is wide, the gear may be classified as "helical-like" rather than "spur-like."

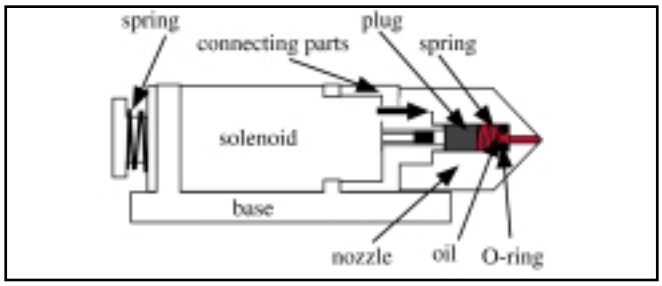

Figure 14—Schematic of the oil shooter.

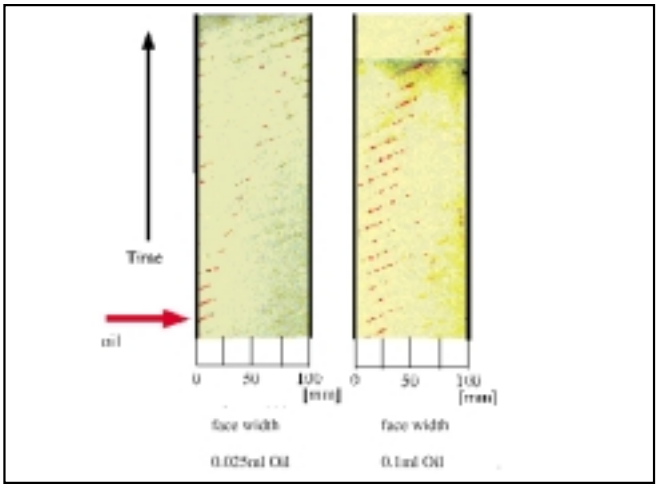

Figure 15—Stamp (red parts) of oil droplet shot from the leading end at the height of about 40 mm from the pitch point. Left: Initial speed is about 13.5 m/s. Right: Initial speed of about 7.5 m/s.

Conclusions

For the purpose of realizing lubrication efficiency improvements, behavior of the medium at the exit of mesh is measured and discussed. The results of this study show that there is an axial travel of strong negative pressures as the meshing proceeds. Also, there is sucking action in the axial direction as well as the concentric direction at the end region of engagement.

References

1. Weiss, T. and M. Hirt, "Efficiency Improvements for High Speed Gears of the 100MW Class," VDI-Berichte 1665, pp. 1161–1174 (2002).
2. Winfree, D.D. "Windage Losses from High Speed Gears," *Proceedings of ASME DETC Conference*, Paper No. PTG-14449 (2000).
3. Houjoh, H., S. Ohshima, S. Miyata, T. Takimoto and K. Maenami, "Dynamic Behavior of Atmosphere in a Tooth Space of a Spur Gear During Mesh Process From the Viewpoint of Efficient Lubrication," *Proceedings of the ASME Design Engineering Technical Conferences*; 2000; Vol. 6, DETC2000/PTG-14372, pp. 111–118.
4. Houjoh, H. and K. Umezawa, "Behavior of an Aerodynamic Sound of Spur Gears (Determination of Similarity Law and Source Locations)," *JSME International Journal Ser. C*, Vol. 36, No. 2, pp. 177–185 (1993).

This paper was originally published by the American Society of Mechanical Engineers at the DET '03 ASME Design Engineering Technical and Computers and Information in Engineering Conference. It can be purchased at the ASME digital store online at *www.asme.org*.